

# False Minutiae’ Impact on Fingerprint Matching: An Investigative Study

Gabriel Babatunde Iwasokun

Department of Web and Multi-Media Computing  
Tshwane University of Technology,  
Pretoria, South Africa  
Email: IwasokunGB {at} tut.ac.za

Oluwole Charles Akinyokun

Department of Computer Science,  
Federal University of Technology,  
Akure, Nigeria

**Abstract**— This paper presents a report on the investigative study of the impact of false minutiae on the performance of fingerprint matching systems. A 3-tier algorithm comprising of pre-processing, minutiae extraction and post-processing stages formed the backbone of the experiments. The pre-processing stage enhanced the fingerprint image, the minutiae extraction stage used the minutiae properties to detect and extract true and false minutiae points while the post-processing stage eliminated the false minutiae points. The experiments were performed on the four datasets in each of the three standard fingerprint databases; namely FVC2000, FVC2002 and FVC2004. The completion times for the minutiae extraction and the post-processing algorithms on each dataset were measured. A standard fingerprint matching algorithm was also implemented for verifying the impact of false minutiae points on FAR, FRR and the matching speed. Analysis of the obtained results revealed that for reliable and optimal performance of fingerprint matching systems, false minutiae points must be eliminated as much as possible from their operations.

**Keywords**- *Fingerprint, minutiae point, AFIS, experimental study, fingerprint databases, fingerprint matching*

## I. INTRODUCTION (HEADING 1)

Automated Fingerprint Identification System (AFIS) is a device for human verification and identification in places or centres where human traffic management and control are required [1-3]. The recent upsurge in the acceptance and use of AFIS over the other biometrics-based devices has been attributed to a number of factors which include:

- Fingerprint exhibits properties that are highly unique from individual to individual
- It is possessed by every individual
- It maintains durable and consistent form in one’s lifetime
- There are a wide range of low-cost devices and technologies for fingerprint enrolment and processing

The steps involved in the operation of an AFIS are conceptualized in Figure 1. For consistent and reliable performance, trust worthy matching or rejection results must be obtained. Very low False Acceptance Rate (FAR) and False Rejection Rate (FRR) are also expected for users’ acceptability and patronage. To achieve these objectives,

suitable and reliable algorithms must form the backbone of these steps.

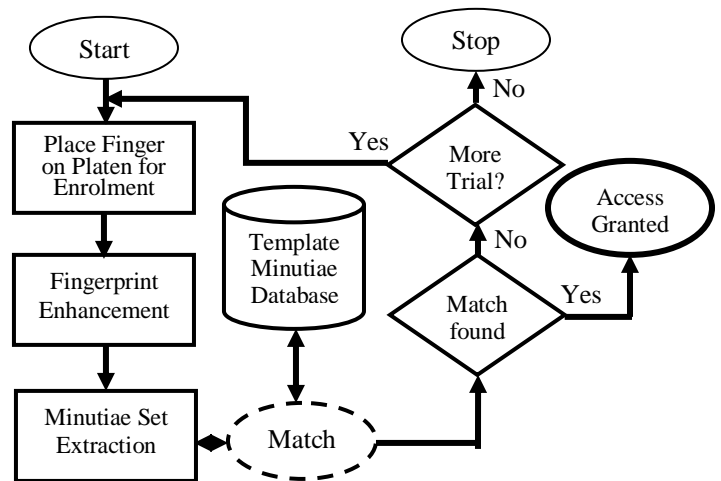


Figure 1: Operational steps of AFIS

Sequel to fingerprint image enrolment, several enhancement activities including pre-processing, segmentation, normalization and image filtering are performed. Local variance and angular definitions constitute the method for fingerprint segmentation to separate the fingerprint foreground from its background. Normalization is also performed for standardization of the ridge grey level values [4]. Several methods including Gabor filter [5-10], Short Time Fourier Transform [11] and Directional Filter [12-14] are some of the most popular approach to filtering fingerprint ridge and valley patterns in gray levels. At the fingerprint enhancement stage, all the noises and the contaminants introduced during enrolment are removed to pave way for a smooth and accurate minutiae extraction. The extracted minutiae then formed the reference minutiae set that is matched with pre-created minutiae sets in the template database. Commonly used minutiae are the end points (enclosed in circles) and bifurcations (enclosed in square) in Figure 2 [15-19]. The ridge terminates at the end point while it splits into two at the bifurcation point.

Based on specified algorithm, the characteristics (orientation, coordinate and distance relative to singular points) for the minutiae set of an image is compared (matched)

with those for other images to establish or reject claim of identity. The implementation of very safe and reliable fingerprint minutiae extraction strategies is therefore important for ensuring accuracy [16-18]. Existing research works on fingerprint minutiae extraction include the use of Adaptive Flow Orientation [19-20], Mathematical Morphology [21-22]; Ridge Tracing [23-24], Fuzzy Image [25] and Complex filtering [26-27]. Others are Weighted Audio Spectrum Flatness-WASF [28], Stochastic Resonance [29], Cellular Neural Networks [30] and Pseudo Zernike Moments [31]. Section 2 of this paper focuses on review of relevant literature while Section 3 presents fingerprint minutiae extraction technique. Sections 4 and 5 present the experimental study and the conclusion respectively.

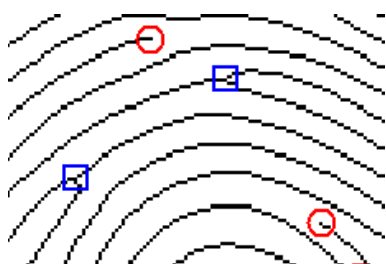


Figure 2: Fingerprint ridges showing end and bifurcation points

## II. LITERATURE REVIEW

Several techniques have emerged for fingerprint minutiae extraction with their respective strengths and weaknesses. The authors in [29] presented a stochastic resonance approach for feature extraction from low-quality fingerprints. Gaussian noise was added to the original fingerprint images earlier rejected due to low-quality by some state-of-the-art fingerprint verification algorithms before extraction. Though, the approach failed with fingerprints with no meaningful features, obtained results showed significant improvement in the equal error and genuine acceptance rates. The authors in [23] presented an algorithm for minutiae extraction from skeletonized and binarized images. An algorithm was also proposed for ridge cleansing based on ridge positions and directional maps. The obtained results showed efficient reduction of spurious minutiae with good performances in dirty areas but the algorithm experiences low processing speed due to computational complexity. The authors in [24] proposed an algorithm for the extraction of fingerprint features from gray scale images by ridge tracing which used contextual information to handle noisy regions with used parameters made adaptive for circumventing human supervision. The algorithm is suitable for speedy extraction of minutiae points but susceptible to extraction of type-exchange minutiae as well as dropped features like short ridges and spurs. Mathematical morphology algorithm is used in [21-22] to remove the superfluous information for genuine feature extraction and measure performance through sensitivity and

specificity. The algorithm effectively removed spurious structures and extracted clear and reliable ridge map from input fingerprint image but experienced a number of missed genuine minutiae. A set of local feature descriptors for fingerprints is proposed in [26]. Minutiae points are detected through a complex filtering of the structure tensor by revealing their positions and directions. Model formulation was by parabolic and linear symmetry descriptions for the extraction of local features and their ridge orientations and reliabilities. Although results on their application in several stages of fingerprint recognition systems showed efficiency, the descriptors failed with severely distorted images. The authors in [30] proposed Cellular Neural Networks (CNN) algorithm for the extraction of high percentage of genuine feature points and their corresponding direction attributes from thinned fingerprint images. The algorithm rejects spurious feature points resulting from noisy fingerprints, but show low computational speed due to un-optimized procedures. A fingerprint local invariant feature extraction using Feature Transform (SIFT) and Speeded-Up Robust Feature (SURF) detectors is proposed in [32]. The detectors run on the central and graphic processing units and focus on the consumed time as important factor for fingerprint identification. The implementations produced promising behaviours for the two detectors with very short processing time.

A method for direct extraction of features from gray-level fingerprint images without binarization and thinning is proposed in [33]. The algorithm traced the ridges, recorded the skeleton image and acquired minutiae with robustness and efficiency. The authors in [15, 17] used Crossing Numbers (CN) algorithms that is based on ridge scanning for fingerprint minutiae extraction. For bad quality image, the algorithm is prone to extraction of exceeding number of false minutiae prompting the authors in [15] to use a post-processing stage to eliminate all forms of spurious features using their ridge and neighbourhood characteristics. A features detection method which reduces the likelihood of an unreliable overlapping region in partial fingerprint is proposed in [34]. The method provides significant improvement for matching low quality images but fails with too much overlapping areas.

A Gabor filter-based method for direct extraction of fingerprint minutiae from grey-level images without pre-processing is proposed in [35]. The method demonstrated efficiency and suitability than other conventional methods but failed with images whose grey-level cannot be determined. The algorithm solved some fingerprint recognition problems relating to translation, scaling and rotation. The authors in [25, 36] implemented algorithms for high level minutiae extraction for all fingerprint images based on pre-processing stages (singular point detection, orientation field estimation and Gabor filter). The performance of these algorithms however depends on the precision of directional and frequency maps. The authors in [31] presented invariant fingerprint minutiae extraction algorithm based on Pseudo Zernike Moments [37-38] and Bayesian classifier [39].

### III. FINGERPRINT MINUTIAE EXTRACTION TECHNIQUE

The algorithm that formed the basis of minutiae extraction experiments is conceptualized in Figure 3 showing the pre-processing, minutiae extraction and validation stages.

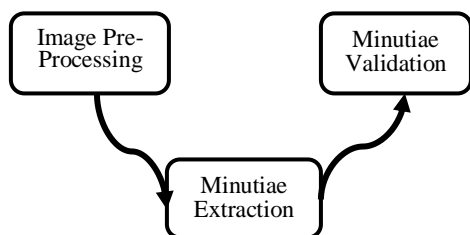


Figure 3: Fingerprint filtering stages

#### A. Image Pre-Processing

For smooth and reliable minutiae extraction, the enrolled fingerprint image is taken through a pre-processing stage of enhancement. The stage includes segmentation, normalization, ridge orientation and frequency estimation, filtering, binarization and thinning. The essence of segmentation is to clearly divide the background region from its foreground region. The background regions generally exhibit high noise and contaminant levels as well as very low grey-scale variance values. On the contrary the foreground regions possess very high variances with minimal noise and contaminants. Based on these characteristics, variance thresholding technique is used to separate the background from the foreground regions. The first step of the technique is a division of the image into blocks followed by the calculation of the grey-scale variance for each block. A block with variance exceeding the global threshold is assigned to the foreground otherwise it is assigned to the background. The grey-level variance for a block,  $b$  with size  $\beta \times \beta$  is defined as [4, 40]:

$$\sigma(b) = \sigma^{-2} \sum_{m=0}^{\beta-1} \sum_{n=0}^{\beta-1} V \quad (1)$$

$$V = (B(m, n) - \mu(b))^2 \quad (2)$$

$\sigma(b)$  is the variance for block  $b$ ,  $B(m, n)$  is the grey-level value at pixel  $(m, n)$ , and  $\mu(b)$  is the mean grey-level value for the block  $b$ .

The segmented image is normalised by regulating its grey-level values to attain uniformity and fall within desired range. If  $\rho(r, s)$  represents the grey-level value at pixel  $(r, s)$ , and  $\beta(r, s)$  represents the normalised grey-level value at pixel  $(r, s)$ , the normalised image is derived from:

$$\beta(r, s) = \begin{cases} \gamma_0 + \sqrt{(\vartheta_0(\rho(r, s) - \gamma)^2)\vartheta^{-1}} & \text{if } \rho(r, s) > \gamma \\ \gamma_0 - \sqrt{(\vartheta_0(\rho(r, s) - \gamma)^2)\vartheta^{-1}} & \text{otherwise} \end{cases} \quad (3)$$

$\gamma$  and  $\vartheta$  are the calculated mean and variance of  $\rho(r, s)$ , respectively while  $\gamma_0$  and  $\vartheta_0$  are the desired mean and variance respectively.

The orientation field of a fingerprint image gives the local orientation of its ridges. It is computed by dividing the image into blocks of uniform sizes and the local orientation for a block with centre at pixel  $(r, s)$  is computed from [40-42]:

$$V_x(r, s) = \sum_{p=r-\frac{W}{2}}^{r+\frac{W}{2}} \sum_{q=s-\frac{W}{2}}^{s+\frac{W}{2}} 2\partial_x(p, q)\partial_y(p, q) \quad (4)$$

$$V_y(r, s) = \sum_{p=r-\frac{W}{2}}^{r+\frac{W}{2}} \sum_{q=s-\frac{W}{2}}^{s+\frac{W}{2}} \partial_x^2(p, q) - \partial_y^2(p, q) \quad (5)$$

$$\theta(r, s) = \frac{1}{2} \tan^{-1} \frac{V_y(r, s)}{V_x(r, s)} \quad (6)$$

$\partial_x(p, q)$  and  $\partial_y(p, q)$  are the gradients obtained using sobel operator at point  $(p, q)$  in  $x$  and  $y$  directions respectively.  $\theta(r, s)$  is the least square estimate of the local orientation of the block with centre at pixel  $(r, s)$ .

The ridge frequency estimation algorithm produces a coarse-level ridge map of the input fingerprint image and it is based on pre-estimated local ridge orientations. Grey levels along fingerprint ridges and valleys are modelled as sinusoidal shaped wave along the normal direction to the local orientation. The wave is principally utilized for the estimation of the ridge frequency based on the assumptions that valid ridge frequencies lie between 1/31 and 1/25 for 500dpi images [6, 43-44]. Fingerprint image filtering is based on the periodic function  $G(x, y; f, \theta)$  as follows [8].

$$G(x, y; f, \theta) = \exp \left[ 0.5 \left[ \frac{\alpha^2 \vartheta_y^2 + \beta^2 \vartheta_x^2}{\vartheta_x^2 \vartheta_y^2} \right] \right] \cos(2\pi f \alpha) \quad (7)$$

$$\alpha = x \sin \theta + y \cos \theta \quad (8)$$

$$\beta = x \cos \theta + y \sin \theta \quad (9)$$

$f$  represents the frequency of the sinusoidal plane wave along the direction  $\theta$  from the  $x$ -axis, and  $\vartheta_x$  and  $\vartheta_y$  are the space constants empirically determined and set to about half the average inter-ridge distance in their respective direction. The filtered image is binarised using the method proposed in [45] to obtain its best performance threshold. The threshold ( $T$ ) is set for making each cluster as tight as possible, thereby minimizing their overlap.  $T$  is determined by separating the pixels into two clusters based on presumed thresholds and the mean of each cluster is determined. The difference between the means is squared and the product of the number of pixels in one cluster and the number in the other is determined. The success of these operations is determined by the difference between the means of the clusters while the optimal threshold maximizes the between-class variance or minimizes the within-class variance. The binarised image is thinned with the Matlab 'bwmorph' operation using the 'thin' option to generate the thin or skeleton image.

**B. Minutiae Extraction**

During minutiae extraction, a fingerprint image is viewed as a flow pattern with a definite texture from which an orientation field for the flow texture is computed [46]. From a filtered (thinned) image, a minutia point is extracted based on its CN value obtained from:

$$CN = \sum_{i=0}^7 |N_{i+2} - N_{i+1}|, \quad N_9 = N_1 \quad (10)$$

$N_1, N_2, \dots, N_8$  represent the 8 neighbours of the candidate minutia point  $N$ , in its  $3 \times 3$  neighbourhood which are scanned in the direction shown in Figure 4.

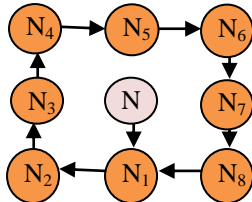


Figure 4: A candidate point and its 8 neighbours

Table I shows the existing CN properties with 2 and 6 denoting ridge end and bifurcation points respectively. These two points are considered as the true minutiae points. The isolated, continuous and crossing points produced spur, hole, triangle and spike structures which are all regarded as false minutiae points. As shown in Figure 5, the spur structure generates false ridge endings while the hole and triangle structures produce false bifurcations. The spike structure also creates a false bifurcation and a false ridge ending point [15, 41, 47]. Figure 6 shows a candidate ridge pixel (at the centre of the enclosed ridges) for ridge ending and bifurcation points.

TABLE I: CN NUMBER AND ITS PROPERTY

S/No.	CN	Property
1	0	Isolated point
2	2	Ridge ending point
3	4	Continuous ridge point
4	6	Bifurcation point
5	8	Crossing point

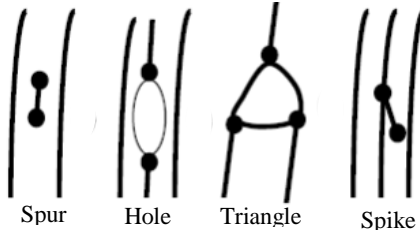


Figure 5: False Minutiae Structures

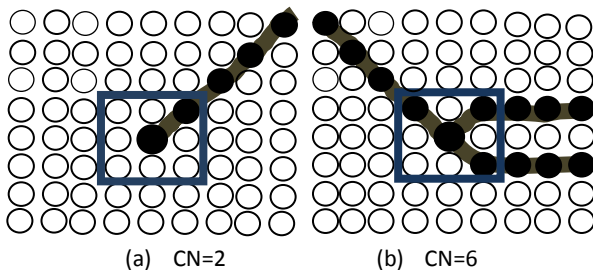


Figure 6: CN values for ridge ending and bifurcation points

**C. Post-Processing**

For the elimination of all forms of false minutiae extracted by the CN algorithm, a post-processing or validation algorithm [15, 20, 40] is implemented. The flowchart of the algorithm is presented in Figure 7. It tests the validity of each candidate minutia point by scanning the skeleton image and examines its local neighbourhood. An image  $M$  of size  $W \times W$  centered on the candidate minutia point is firstly created and its central pixel is labelled with CP while the remaining pixels are initialised to zero. Other connecting point is labelled with 1 and 3 for ridge end and bifurcation points respectively as shown in Figure 8.

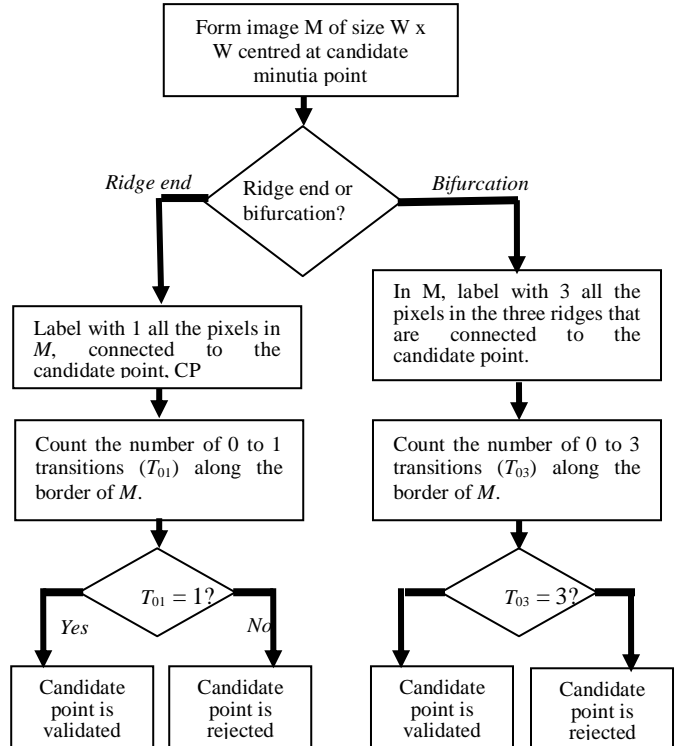


Figure 7: Flowchart for minutiae validity test

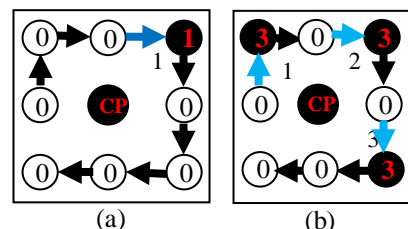


Figure 8: 0 to 1 transitions. (a) Bifurcation ( $T_{03}=3$ ), (b) Ridge ending ( $T_{01}=1$ )

**IV. EXPERIMENTAL STUDY**

The experiments based on Matlab application were carried out using FVC2000, FVC2002 and FVC2004 standard fingerprint databases on Ms-Windows 7 Operating System on a Pentium 4 – 2.80 GHz dual processors with 4.00GB of RAM. The summary of the three standard databases is presented in



Table II [48-49]. The three databases were jointly formulated by the Biometric System Laboratory of the University of Bologna, together with the Biometric Test Centre of the San Jose State University and the Pattern Recognition and Image Processing Laboratory of the Michigan State University. There are four datasets in each of the three databases and each dataset has 80 fingerprints of different qualities and obtained at different resolution, orientation and sizes on the basis of 8 enrolments from each of 10 different people.

Figures 9(d), 9(e) and 9(f) present the extracted minutiae based on CN algorithm from the skeleton (thinned) images of Figure 9(a), 9(b) and 9(c) respectively. The true ridge ends points are shown with circles (red colour), the square marks (blue colour) represent the true bifurcation points and the false minutiae points are denoted with diamonds (in green). The ratio of true to false ridge end points extracted and shown in Figure 9(d), 9(e) and 9(f) are 19:13, 25: 14 and 26: 13 respectively. For bifurcation points, the ratio is 13:7, 6:13 and

TABLE II: DETAILS OF THE STANDARD FINGERPRINT DATABASES

Data-base	Sensor Type			Image size			No.	Resolution		
	FVC2000	FVC2002	FVC2004	FVC2000	FVC2002	FVC2004		FVC2000	FVC2002	FVC2004
DB1	Optical Sensor			300 x 300	388 x 374	640 x 480	100 x 8	500 dpi	500 dpi	500 dpi
DB2	Capacitive Sensor	Optical Sensor		256 x 354	296 x 560	328 x 364	100 x 8	500 dpi	569 dpi	500 dpi
DB3	Optical Sensor	Capacitive Sensor	Thermal Sweeping	448 x 478	300 x 300	300 x 480	100 x 8	500 dpi	500 dpi	512 dpi
DB4	SFinGe v2.0	SFinGe v2.51	SFinGe v3.0	240 x 320	288 x 384	288 x 384	100 x 8	About 500 dpi	About 500 dpi	About 500 dpi

TABLE III: STATISTICS OF EXTRACTED TRUE AND FALSE MINUTIAE FROM THE THREE DATABASES

Dataset		FVC2000		FVC2002		FVC2004	
		Total	Time(s)	Total	Time(s)	Total	Time(s)
DB1	Ridge end	10683	91.86	6980	119.01	10822	200.20
	Bifurcation	6254		9545		12389	
DB2	Ridge end	7914	97.05	22425	158.93	14962	114.37
	Bifurcation	8008		14156		11276	
DB3	Ridge end	54165	231.34	13124	91.81	18198	133.95
	Bifurcation	46681		15676		12565	
DB4	Ridge end	6269	73.35	17735	97.95	14544	100.32
	Bifurcation	8147		12873		12137	

The detailed results for the pre-processing sub-stages of segmentation, normalization, filtering, binarization and thinning had been discussed in [50] and they are excluded from this report. Formatted images from datasets DB1 of FVC2000, FVC2002 and FVC2004 standard databases are shown in Figure 9 (a), 9(b) and 9(c) respectively.

9:19 respectively. The results from the minutiae extraction experiments on the three standard fingerprint databases using the CN algorithm are presented in Table III. Higher values are recorded for false minutiae points over true minutiae points in all cases. As shown in Figures 10 and 11, there are higher percentages for false ridge end and bifurcation points in all the datasets and databases.

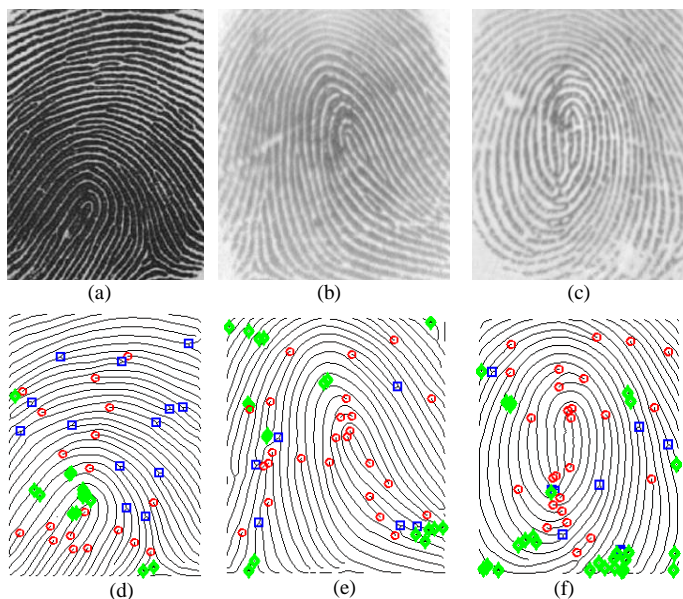


Figure 9: Fingerprint images from standard databases and their true and false minutiae points

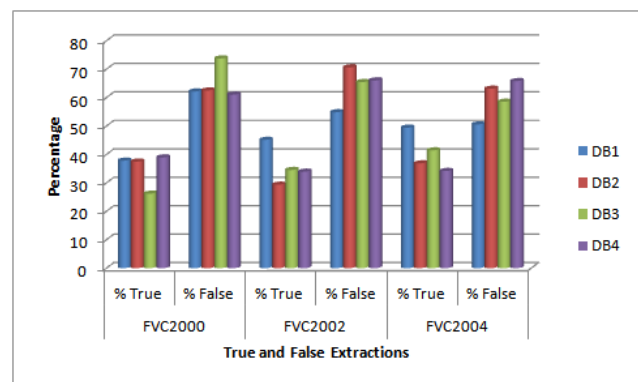


Figure 10: Percentage of true and false extracted ridge ends

The exceedingly higher number of extracted false minutiae points is attributed to the presence of high cases of corrupted

regions in several of the images. The corrupted regions resulted in the introduction of a great number of artifacts during enhancement [3] some of which appear in form of ridge ends while others as bifurcations. In Figure 12, a highly corrupted image in dataset DB3 of FVC2000 fingerprint database is presented with its extracted true and false minutiae points (marked with 'X') with numerous overlaps, outnumbered the true minutiae points (shown in circles and squares). A total of 123 false minutiae extraction is recorded as against 59 for true minutiae points.

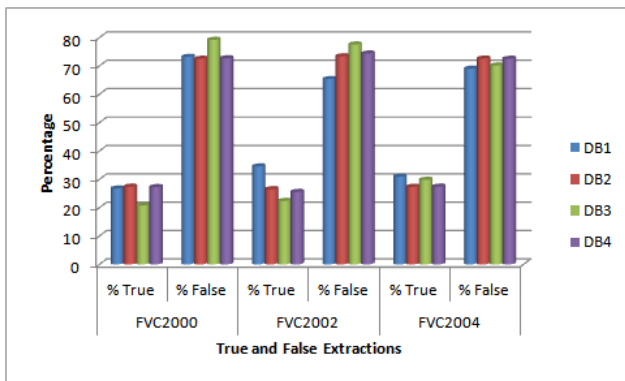


Figure 11: Percentage of true and false extracted bifurcations

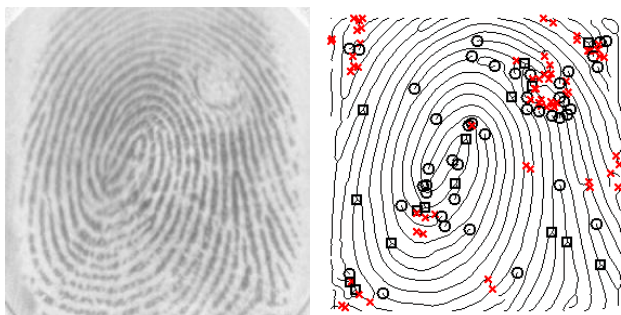


Figure 12: Fingerprint image and its extracted true and false minutiae points

Since different enrolment (from same or different fingers) experience different level of corruption (noise and contaminations), it is therefore consequential that different number of true and false minutiae points will be generated for different images. It also implied that the extraction of different number of false minutiae from images of the same finger will pose a great challenge to reliable implementation of AFIS. Using a window size of 23 x 23, the post-processing algorithm experiments were used to achieve total elimination of all false minutiae points and the results for Figures 9(d), 9(e) and 9(f) are shown in Figure 13(a), 13(b) and 13(c) respectively. The summary of the results of the elimination of all false minutiae points from the images in the three databases are presented in Table IV. The summary shows very significant reduction in the number of extracted minutiae but increase in the completion time when compared with Table III. The increase in the completion time is the time for the extra effort of validating or rejecting a minutia point.

TABLE IV: STATISTICS OF EXTRACTED TRUE MINUTIAE FROM THE THREE DATABASES

Dataset		FVC2000		FVC2002		FVC2004	
		Total	Time(s)	Total	Time(s)	Total	Time(s)
DB1	Ridge end	4042	99.88	3151	38.01	5349	210.17
	Bifurcation	1675		3302		3832	
DB2	Ridge end	2966	104.15	6587	59.93	5515	126.34
	Bifurcation	2197		3759		3088	
DB3	Ridge end	14200	254.38	4532	42.81	7543	143.98
	Bifurcation	9694		3510		3750	
DB4	Ridge end	2442	79.86	6021	58.95	4972	110.89
	Bifurcation	2223		3293		3331	

Window size exceeding or below the stated value showed some deficiencies in the elimination of the false minutiae points [15]. When the window size is higher, some false minutiae points are extracted while lower value led to the non-extraction of some valid minutiae points.

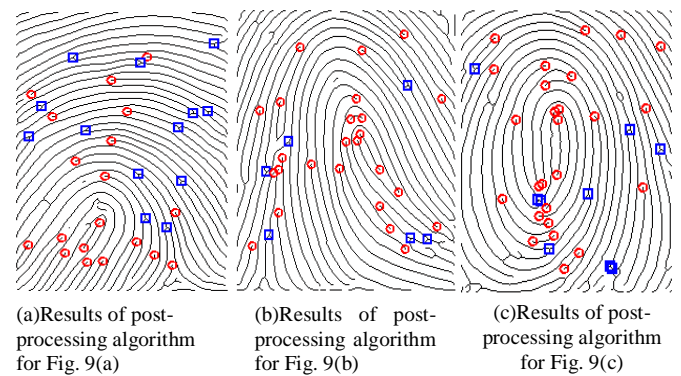


Figure 13: Results showing the elimination of false minutiae

Experiments were also conducted for the evaluation of the impact of the false minutiae points on fingerprint matching. Based on the algorithm proposed in [51], false rejection and acceptance rates experiments were performed on fingerprints in the three databases. The false acceptance experiments measured the rate at which images from different fingers are found to match (matching value exceeding threshold). The false rejection experiments also measured the rate at which images from same finger failed to match (matching value falling below threshold). In all the datasets, matching experiments based on minutiae extracted using CN algorithm (which produced true and false minutiae) in one hand and post-processing algorithm (which produced only true minutiae points) on the other hand, resulted in False Acceptance Rate (FAR) of 0%. The trend of obtained False Rejection Rate (FRR) results for the two sets of experiments is presented in Figure 14. The lower FRR values for true minutiae-based matching indicate there is greater accuracy, reliability and efficiency when false points are eliminated from the minutiae set. The higher FRR values for matching inclusive of false minutiae points imply that the presence of false minutiae points is capable of worsening the performance of a fingerprint matching algorithm.

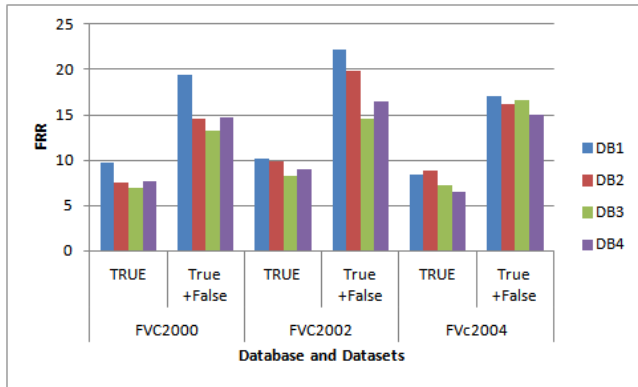


Figure 14: FRR results for matching with and without false minutiae points

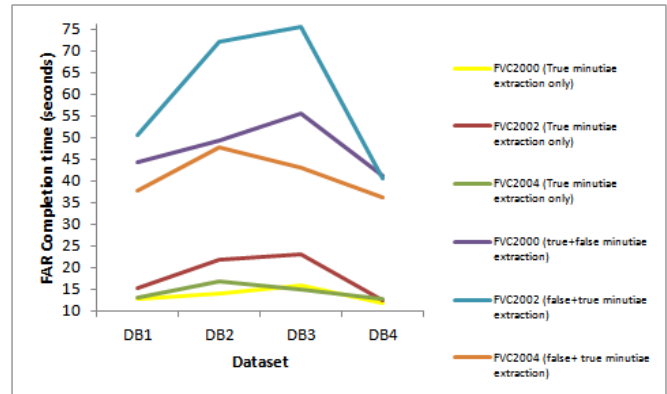


Figure 15: Line plot of the FAR completion times

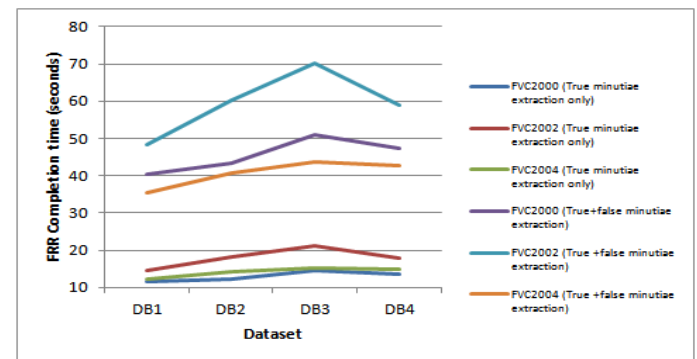


Figure 16: Line plot of the FRR completion times

The completion times (in seconds) for FAR and FRR experiments on the 80 fingerprint images in each of the datasets for every standard database are shown in Tables V and VI. Based on the figures presented on these Tables, the line plots of Figure 15 and 16 clearly show the very wide gaps between the computation times for FAR and FRR in the CN and post-processing algorithms-based experiments. The lower completion times for the post-processing-based experiments are attributed to lower number of minutiae searches and minimum computations. Statistical analysis of the values presented in Tables V and VI also revealed that matching inclusive of false minutiae points take about 3.5, 3.29 and 2.86 times the time for true minutiae-based matching for all the datasets in FVC2000, FVC2002 and FVC2004 standard databases respectively. It is therefore obvious that the elimination of all false minutiae points at the feature extraction stage in a fingerprint pattern matching system is a necessity for reliable, high speed and user friendly operation.

TABLE V: COMPLETION TIME (IN SECONDS) FOR TRUE MINUTIAE-BASED FINGERPRINT MATCHING

	FVC2000		FVC2002		FVC2004	
	FAR	FRR	FAR	FRR	FAR	FRR
DB1	12.62	11.51	15.33	14.65	13.14	12.36
DB2	14.11	12.37	21.92	18.31	16.70	14.21
DB3	15.90	14.52	22.91	21.33	15.01	15.32
DB4	11.73	13.57	12.34	17.95	12.62	14.94

TABLE VI: COMPLETION TIME (IN SECONDS) FOR FINGERPRINT MATCHING INCLUSIVE OF FALSE MINUTIAE

Data set	FVC2000		FVC2002		FVC2004	
	FAR	FRR	FAR	FRR	FAR	FRR
DB1	44.17	40.28	50.43	48.19	37.58	35.34
DB2	49.38	43.29	72.11	60.23	47.76	40.64
DB3	55.65	50.82	75.37	70.17	42.92	43.81
DB4	41.05	47.49	40.59	59.05	36.09	42.72

## V. CONCLUSION

This paper presented a report on the experimental study of the impact of false minutiae points on the performance of AFIS. A 3-tier algorithm was implemented with the results at each level showing relevance and meaningfulness. Results for fingerprint minutiae extraction algorithm revealed its inability to enforce the extraction of only true minutiae points. At the post-processing stage, only the true minutiae points; namely ridge end and bifurcation were extracted. Analysis of experimental results for both feature extraction and post-processing algorithms on FVC2000, FVC2002 and FVC2004 fingerprint databases revealed that for speedy and reliable performance of AFIS, all forms of false minutiae points must be eliminated from its operation.

## REFERENCES

- [1] Robert Carrigan, Ron Milton, Dan Morrow (2005), Automated Fingerprint Identification Systems, Computer world Honours: Case Study ([www.cwhonors.org/archives/case\\_studies/Axiom.pdf](http://www.cwhonors.org/archives/case_studies/Axiom.pdf)). Accessed 12/011/2013
- [2] Zhang Jinhai, Liu Xinjian, Chen Bo (2011), The design and implementation of ID Authentication System Based on Fingerprint Identification, Proc. of Fourth International Conference on Intelligent Computation Technology and Automation ([kresttechnology.com](http://kresttechnology.com)). Accessed 16/12/2013
- [3] Jain Anil K., Salil Prabhakar, Shaoyun Chen (1999), Combining Multiple matchers for a High Security Fingerprint Verification System, Pattern Recognition Letters Volume 20, pages 1371-1379

- [4] Iwasokun G. B., O. C. Akinyokun & O. Olabode (2012): A Mathematical Modelling Approach to Fingerprint Ridge Segmentation and Normalization, International Journal of Computer Science and Information Technology & Security, Singapore, Vol. 2, No. 2, page 263-267
- [5] Pannirselvam S. and P. Raajan (2012), An Efficient Fingerprint Enhancement Filtering Technique with High Boost Gaussian Filter (HBG), International Journal of Advanced Research in Computer Science and Software Engineering, Vol. 2, issue 11
- [6] Hong, L., Wan, Y. and Jain, A. (1998), Fingerprint Image Enhancement: Algorithm and Performance Evaluation. IEEE Transactions on Pattern Analysis and Machine Intelligence Vol. 20, pages 777–789
- [7] Yang Jianwei, Lifeng Liu, Tianzi Jiang, Yong Fan (2003), A Modified Gabor Filter Design Method for Fingerprint Image Enhancement, Pattern Recognition Letters, Volume 24, pages 1805–1817
- [8] Hongchang Ke1, a, Hui Wang2, b and Degang Kong (2012), An Improved Gabor Filtering for Fingerprint Image Enhancement Technology, Proceedings of the 2nd International Conference on Electronic & Mechanical Engineering and Information Technology (EMEIT-2012)
- [9] Dhanabal R., V. Bharathi, G. Prithvi Jain, Ganeash Hariharan, P. Deepan Ramkumar Sarat Kumar Sahoo (2013), International Journal of Engineering and Technology (IJET), Vol 5, Issue 2
- [10] Prajakta M. Mudegaonkar, Prof. Ramesh P. Adgaonkar (2011), A Novel Approach to Fingerprint Identification Using Gabor Filter-Bank, ACEEE International Journal on Network Security, Vol. 02, No. 03
- [11] Chikkerur Sharat, Venu Govindaraju, and Alexander N. (2005), Fingerprint Image Enhancement Using STFT Analysis, S. Singh et al. (Eds.): ICAPR 2005, LNCS 3687, pp. 20–29, 2005.
- [12] Sherlock, B.G., Monroe, D.M., Millard, K. (1994), Fingerprint Enhancement by Directional Fourier Filtering, IEE Proc. Vision Image Signal Process volume 141, Issue 2, pages 87–94.
- [13] Aarthy V., R. Mythili, M. Mahendran (2012), Low Quality Fingerprint Image Using Spatial and Frequency Domain, International Journal of Computational Engineering Research Vol. 2 Issue 6.
- [14] Josef Strom Bartunek, Mikael Nilsson, Jorgen Nordberg, and Ingvar Claesson (2006), Adaptive Fingerprint Binarization by Frequency Domain Analysis, 1424407850/06/\$20.00
- [15] Iwasokun G. B., O. C. Akinyokun, B. K. Alese & O. Olabode (2011), Adaptive and Faster Approach to Fingerprint Minutiae Extraction and Validation. International Journal of Computer Science and Security, Malaysia, Volume 5 Issue 4, page 414-424
- [16] Babasaheb V. Bhalerao, Ramesh R. Manza (2013), Development of Image Enhancement and the Feature Extraction Techniques on Rural Fingerprint Images to Improve the Recognition and the Authentication Rate, IOSR Journal of Computer Engineering (IOSR-JCE), Volume 15, Issue 1, Pages 01-05 ([www.iosrjournals.org](http://www.iosrjournals.org) [www.iosrjournals.org](http://www.iosrjournals.org))
- [17] Nalini K. Ratha, Shaoyun Chen and anil K. Jain (1995), Adaptive Flow Orientation-based Feature Extraction in Fingerprint Images, Pattern Recognition, Volume 28, Number 11, Pages 1657-1672
- [18] Moses Kenneth R., Peter Higgins, Michael McCabe, Salil Prabhakar, Scott Swann, Automated Fingerprint Identification System (AFIS), (Unpublished) (<https://www.ncjrs.gov/pdffiles1/nij/225326.pdf>). Accessed 01/11/2013
- [19] Ratha N., Chen S. and Jain A. K. (1995), Adaptive Flow Orientation Based Feature Extraction in Fingerprint Images, Pattern Recognition, Vol. 28, No. 11, pp. 1657-1672.
- [20] Kasaei Shohreh, Mohamed Deriche and Boualem Boashash, Fingerprint Feature Enhancement using Block Direction on Reconstructed Image, (Unpublished) ([sina.sharif.edu/~skasaei/Papers/icics02.pdf](http://sina.sharif.edu/~skasaei/Papers/icics02.pdf)). Accessed 07/02/2014
- [21] Humbe Vikas, S. S. Gornale, Ramesh Manza & K. V. Kale (2007), International Journal of Computer Science and Security, Volume 1, Issue 2
- [22] Shevaani Garg, Suman Thapar (2012), Feature extraction using Morphological Operations on Fingerprint Images, International Journal of Computing and Business Research ([www.researchmanuscripts.com/isociety2012/40.pdf](http://www.researchmanuscripts.com/isociety2012/40.pdf)). Accessed 12/01/2014
- [23] Farina Alessandro, Zsolt M. Kovacs-Vajna, Alberto Leone (1999), Fingerprint Minutiae Extraction from Skeletonised Binary Images, Pattern Recognition, Volume 32
- [24] Devansh Arpit and Anoop Namboodiri (2011), Fingerprint Feature Extraction from Gray Scale Images by Ridge Tracing, 978-1-4577-1359-0/11/\$26.00 IEEE
- [25] Surmacz Kamil, Khalid Saeed, Piotr Rapta (2011), An Improved Algorithm for Feature Extraction from a Fingerprint Fuzzy Image, Optica Applicata, Vol. XLIII, No. 3, DOI: 10.5277/oa130311
- [26] Hartwig Fronthaler, Klaus Kollreider and Josef Bigun (2005), Local Feature Extraction in Fingerprints by Complex Filtering, S.Z. Li et al. (Eds.): IWBR 2005, LNCS 3781, pp. 77–84, Springer-Verlag Berlin Heidelberg
- [27] Chih-Jen Lee and Sheng-De Wang (1999), Fingerprint Feature Extraction Using Gabor Filters, Electronic Letters, Volume 35, Number 4
- [28] Chen Jianping, Huang Tiejun (2008), A Robust Feature Extraction Algorithm for Audio Fingerprinting (<http://159.226.42.3/doc/2008/A%Robust%Feature%Extraction%Algorithm%for%Audio%Fingerprinting.pdf>). Accessed 09/02/2014
- [29] Ryu Choonwoo, Seong G. Kong, Hakil Kim (2011), Enhancement of Feature Extraction for Low-quality Fingerprint Images Using Stochastic Resonance, Pattern Recognition Letters, Volume 32, Pages 107-113
- [30] Gao Qun and George S. Moschytz (2001), Fingerprint Feature Extraction Using CNNs, Proceedings of European Conference on Circuit Theory and Design, August 28-31, 2001, Espoo, Finland
- [31] Deepika C.Lakshmi, Dr. A Kandaswamy, C. Vimal, and B. Sathish (2010), Invariant Feature Extraction from Fingerprint Biometric Using Pseudo Zernike Moments, Singaporean Journal Scientific Research (SJSR), 0061 Vol.3, No.2 pp.150 – 154, <http://www.iaaet.org/sjsr>
- [32] Awad Ali Ismail (2013), Fingerprint Local Invariant Feature Extraction on GPU with CUDA, Informatica Volume 37, Pages 279–284
- [33] Yang Jianwei, Lifeng Liu and Tianzi Jiang (2001), An Improved Method for Extraction of Fingerprint Features ([nlprweb.ia.ac.cn/English/mic/jianweiyang/ICIG\\_yang.pdf](http://www.iaaet.org/sjsr)), Accessed 10/02/2014
- [34] Nathaniel J. Short (2012), Robust Feature Extraction and Temporal Analysis for Partial Fingerprint Identification, PhD Thesis (unpublished) submitted to the Faculty of the Virginia Polytechnic Institute and State University
- [35] Chih-Jen Lee and Sheng-De Wang (1999), Fingerprint Feature Extraction Using Gabor Filters, Electronic Letters, Volume 35, Number 4
- [36] Meenakshi Awasthi and Ajay Sharma (2012), An Efficient Algorithm for Minutiae Feature Extraction Method, VSRD International Journal of Electrical, Electronic and Communication Engineering, Vol. 2, Issue 8, pages 585-593
- [37] Teague M.R., Image Analysis via the general theory of moments, Journal of Optical, Society., Volume 23, 1975.
- [38] The C. H, Chin R. T.(1988), On Image Analysis by the Methods of Moments, IEEE Transactions on Pattern Analysis Machine Intelligent, Vol. 10, No. 4, page. 496- 513.
- [39] Siavash Mirarab, AlaaHassouna, LadanTahvildari (2007), Using Bayesian Belief Networks to Predict Change Propagation in Software Systems, Proceeding of IEEE 15th International Conference on Program Comprehension (ICPC '07) page 177-188.
- [40] Hong Liu, Wau Yifei and Anil Jaiu (2006), Fingerprint Image Enhancement: Algorithm and Performance Evaluation, Pattern Recognition and Image Processing Laboratory, Department of Computer Science, Michigan State University, pages1-30
- [41] Raymond Thai (2003), Fingerprint Image Enhancement and Minutiae Extraction, PhD Thesis (Unpublished) Submitted to School of Computer Science and Software Engineering, University of Western Australia, pp21-56.
- [42] Iwasokun G. B., O. C. Akinyokun & O. Olabode (2012), A Block Processing Approach to Fingerprint Ridge Orientation Estimation, Journal of Computer Technology and Application, USA, Volume 3, Pages 401-407.



- [43] Arun Vinodh C. (2007), Extracting and Enhancing the Core Area in Fingerprint Images, IJCSNS International Journal of Computer Science and Network Security, VOL. 7 No. 11, pages 16-20.
- [44] Iwasokun G. B., O. C. Akinyokun & O. Olabode (2013), Uniformity Level Approach to Fingerprint Ridge Frequency Estimation, International Journal of Computer Applications, USA, Volume 61, Number 22, pages 26-32.
- [45] Liang, Xu (2009), Image Binarization using Otsu Method, Proceedings of NLPR-PAL Group CASIA Conference, pages 345-349
- [46] Sudha S. Ponnarasi and M. Rajaram (2012), Impact of Algorithms for the Extraction of Minutiae Points in Fingerprint Biometric, Journal of Computer Science Vol. 8, No. 9, pages 1467-1472
- [47] Xiao, Q. and Raafat, H. (1991), Fingerprint image Post-processing: A Combined Statistical and Structural Approach, Pattern Recognition Vol. 24, Issue 10 pages 985–992
- [48] Cappelli R, Maio D., Maltoni D., Wayman J. L. and A. K. Jain (2006), Performance Evaluation of Fingerprint Verification Systems, IEEE Transactions on Pattern Analysis and Machine Intelligence, Vol. 28 NO. 1, pp. 3 - 18.
- [49] Jiangang Cheng, Jie Tian (2004), Fingerprint Enhancement with Dyadic Scale-Space, Pattern Recognition Letters, Elsevier B.V
- [50] Iwasokun G. B., O. C. Akinyokun, C. O. Angaye and O. Olabode (2012), A Multi-Level Model for Fingerprint Enhancement, Journal of Pattern Recognition Research, USA, Vol. 7 pages 155-174
- [51] Iwasokun G. B., O. C. Akinyokun and C. O. Angaye (2013), Fingerprint Matching using Neighbourhood Distinctiveness, International Journal of Computer Applications, USA, Volume 66, No. 21.